EUROPEAN ORGANIZATION FOR NUCLEAR RESEARCH

CERN-EP/99-04
28.01.1999

Particle-hole excitations in the interacting boson model (IV) : The U(5)-SU(3) coupling

C. De Coster[1,*], B. Decroix[1], K. Heyde[1,2], J. Jolie[3], H. Lehmann[4], J.L. Wood[5]

[1] *Vakgroep Subatomaire en Stralingsfysica, Proeftuinstraat 86, B-9000 Gent, Belgium*
[2] *present address: EP-ISOLDE, CERN, CH-1211 Geneva 23, Switzerland*
[3] *Institut de Physique, Université de Fribourg, Pérolles CH-1700 Fribourg, Switzerland*
[4] *Institut Laue-Langevin, BP 156, 38042 Grenoble CEDEX, France*
[5] *School of Physics, Georgia Institute of Technology, Atlanta, Georgia 30332-0430, U.S.A*
[*] *postdoctoral research fellow of the Fund for Scientific Research - Flanders (Belgium)*

Abstract

In the extended interacting boson model (EIBM) both particle- and hole-like bosons are incorporated to encompass multi-particle-multi-hole excitations at and near to closed shells. We apply the group theoretical concepts of the EIBM to the particular case of two coexisting systems in the same nucleus exhibiting a U(5) (for the regular configurations) and an SU(3) symmetry (for the intruder configurations). Besides the description of "global" symmetry aspects in terms of I-spin , also the very specific local mixing effects characteristic for the U(5)-SU(3) symmetry coupling are studied. The model is applied to the Po isotopes and a comparison with a more realistic calculation is made.

PACS: 21.60.Ev; 21.60.Fw; 24.80.Dc
Keywords: Particle-hole excitations; I-spin multiplets; U(5)-SU(3) coupling.

(ISOLDE GENERAL)

(submitted to Nuclear Physics A)

1 Introduction

In the present series of articles, concentrating on the various possibilities that show up when introducing particle and hole bosons explicitly within an extended interacting boson model approach (EIBM), we have studied, besides the general formalism (part I, ref. [1]) those situations where – as a manifestation of K-symmetry breaking – intruder multi-particle-multi-hole and regular excitations are described by different dynamical symmetries in an IBM-1 framework as a limiting case, i.e., the U(5)-O(6) coupling (part II, ref. [2]) and the O(6)-SU(3) coupling (part III, ref. [3]). We concentrated also on nuclei where those symmetries appear (approximately), i.e., in the Sn and Pb region, respectively.

In the present article (part IV) we study those cases where the regular states are described by a U(5) symmetry but the intruder states form rotational structures best approximated by an SU(3) symmetry. Besides discussing in section 2.1 the data which may indicate the presence of such dynamical symmetries, we study in detail the pure U(5)-SU(3) model in section 2.2. More specifically we study the coupling that may arise in actual nuclei between these two symmetries both in a numerical and an analytical way, trying to understand the specific mixing features. In section 2.3 we discuss the mixing of the wave functions of the combined system and its implications on the B(E2) values for the lowest lying states occurring in the two symmetries. In section 2.4 we point out how to go from this limiting case gradually into more realistic cases.

In section 3 we discuss how the above symmetry conditions may well be showing up, albeit approximately, in the Po isotopes, with implications for the observation of intruder analog multiplets. In the concluding section 4 we summarize the effects of the various symmetries and their most salient features discussed in previous articles (part II, III and IV).

2 The U(5)-SU(3) coupling

2.1 Experimental evidence for U(5)-SU(3) coexisting systems

When discussing in part II the experimental evidence for the appearance of U(5) regular excitations and O(6) intruder excitations in the Cd nuclei, we have pointed out that the global symmetry character can change in a smooth way. It seems that when going from the Cd nuclei (two proton holes in the Sn core) across the Z=50 closed shell into the Te nuclei (two proton particles outside the Sn core), the global intruder symmetry is changing in character from an O(6) symmetry into an SU(3) symmetry. Some consequences of such a smooth O(6)-SU(3) transition have been studied recently [4].

However, in contrast with the nearby Cd nuclei having the same neutron number N, the even-even Te nuclei show no clear-cut evidence of well-deformed intruder bands. Still, this mass region, where the valence proton character is particle-like (Z $\rangle$ 50) and where the neutron number appears around the midshell (N = 66) configuration, may well be an appropriate mass region to find an approximate realization of the U(5)-SU(3) coupling. ^{118}Te seems to be the best case so far [5]. A systematic analysis of the experimental data for $^{112-128}$Te combined with a mixed configuration IBM-2 calculation [6] suggests a strong intruder admixture. Still it is stated that the underlying vibrational normal excitation

structures do not closely approach any of the dynamical symmetry limits of the IBM. We will therefore not concentrate on this region but refer the reader to the above analysis.

We suggest that in the Pb region (Z=82), this particular symmetry classification might well be present. The spectra of the even-even Po nuclei (Z=84) evolve from typical two-particle shell-model spectra near N=126 over transitional into anharmonic quadrupole vibrational characteristics when approaching the neutron deficient region [7]-[19]. At the same time, even though two-particle-core coupling studies can account for the quadrupole anharmonic structures [10]-[13], a conspicuous onset of a low-lying 0^+ level, dropping rapidly in excitation energy from ^{202}Po onwards, has been observed. By now, the evidence seems rather compelling that indeed an intruder band is dropping rapidly in excitation energy when approaching the mid-shell region (N=116 $\rightarrow$ 108) [14]-[19]. So, it looks like an SU(3) structure is appearing next to the regular anharmonic quadrupole vibrational excitations in this mass region, even becoming the ground band in ^{192}Po [20].

The Po region then appears on equal footing with the Te mass region for which the above symmetries – although in an approximate way – have also been suggested. In both cases we have two proton particles outside the closed shell (Z=52 in the Te nuclei, Z=84 in the Po nuclei) and in each case going together with a neutron number near or slightly above the neutron mid-shell configuration. The energy systematics for the Po nuclei as well as their interpretation in terms of mixed regular and intruder bands are given in figs. 1 a and b, respectively.

2.2 The pure U(5)-SU(3) model

In analogy to what has been done in part II and III, here it is assumed that the normal configuration can be described by the pure U(5) dynamical symmetry limit of the IBM with no admixture of the other dynamical symmetry limits. The eigenstates of such a system can be written as:

$$|[N], n_d, v, L\rangle \quad , \tag{1}$$

with n_d, v and L the U(5), O(5) and O(3) quantum numbers. In order to describe the extra states due to the proton-pair excitations across the closed shell it is necessary to include a second set of configurations. These configurations are assumed to be more deformed and are approached as being governed by the SU(3) dynamical symmetry with two additional bosons to encompass the 2p-2h excitations in addition to the normal configuration. The eigenstates are given by:

$$|[N+2], (\lambda, \mu), L\rangle \quad , \tag{2}$$

with (λ, μ), L the SU(3) and O(3) quantum numbers. In general, one expects the global structure to be reproduced by these two coexisting configurations, i.e., the U(5) and SU(3) states, as shown in fig. 2, with an offset of $\Delta + \langle \hat{Q} \cdot \hat{Q} \rangle$. Here Δ is a parameter which accounts for the energy shift due to the promotion of two particles across the closed shell, which the IBM cannot explicitly account for, i.e., the single-particle-energy difference with the pairing and monopole energy shifts added [2]. The lowering of the intruder configuration when approaching midshell is caused predominantly by the proton-neutron quadrupole interaction $\hat{Q}_\pi \cdot \hat{Q}_\nu$, which is explicitly accounted for in the IBM diagonalization.

One expects that, in regions where intruder and regular configurations come close in energy, detailed spectra and especially wave-function sensitive (and so more local) properties like B(E2) values, will reflect K-mixing of these coexisting systems, as was clearly shown in part II. In the latter paper, the interaction was introduced in its more general form. To first order, it takes the following (IBM-1) form [2, 21]:

$$\hat{H}_{mix} \;=\; \alpha\,[s^{\dagger}s^{\dagger}+ss]^{(0)} + \beta\,[d^{\dagger}d^{\dagger}+\tilde{d}\tilde{d}]^{(0)} \quad . \tag{3}$$

This basic coupling structure leads to the following form of the energy matrix:

$$\left(\begin{array}{c|c} U(5)_N & \langle U(5)_N|\hat{H}_{mix}|SU(3)_{N+2}\rangle \\ \hline \langle SU(3)_{N+2}|\hat{H}_{mix}|U(5)_N\rangle & SU(3)_{N+2} \end{array}\right); \tag{4}$$

where $U(5)_N$ and $SU(3)_{N+2}$ are the eigenvalues in the corresponding dynamical symmetry limit which, in their most general form, are given by [22]

$$\begin{aligned} U(5)_N \;&=\; \epsilon''' n_d + \alpha_{U5} n_d(n_d+4) + \beta_{U5} 2v(v+3) + \gamma_{U5} 2L(L+1)\;, \\ SU(3)_{N+2} \;&=\; \Delta \;+ \delta\frac{2}{3}(\lambda^2+\mu^2+\lambda\mu+3\lambda+3\mu) + \gamma_{SU3} 2L(L+1)\;. \end{aligned} \tag{5}$$

and $\langle U(5)_N|\hat{H}_{mix}|SU(3)_{N+2}\rangle$ is the interaction between the two configurations governed by the mixing Hamiltonian given in (3). The parameter Δ, which shifts the intruder states to higher energies as mentioned before, is explicitly included here.

Contrary to the U(5)-O(6) model [21], where both dynamical symmetries have a common O(5) $\supset$ O(3) subgroup chain [23], no clear-cut selection rules that govern the coupling between the U(5)-SU(3) dynamical symmetries show up. So, one can expect a very different coupling pattern, as was already indicated when studying the effect of the O(6) $\rightarrow$ SU(3) symmetry transition on the coupling [4]. In the more general case, one needs to expand the SU(3) states in the U(5) basis, in which the mixing matrix elements can be most easily calculated. However, because of the appearance of missing labels in both the U(5) and SU(3) wave functions, it is difficult to derive general analytic expressions for the transformation brackets

$$\langle [N](\lambda,\mu)L \mid [N] n_d, v, L\rangle \quad . \tag{6}$$

The one exception is the SU(3) ground state (2N,0)L=0 for which no multiplicity is present and for which the transformation bracket has the explicit form

$$\begin{aligned} &\langle [N] n_d v 00 \mid [N](2N,0)00\rangle = \\ &\quad \left[\frac{2^{n_d+v+1}(2N+1)(2v+3)N!((n_d+v)/2+1)!}{3^N(N-n_d)!((n_d-v)/2)!(n_d+v+3)!}\right]^{1/2} \quad . \end{aligned} \tag{7}$$

The transformating bracket (7) is equivalent to the one derived in [24] apart from the phasefactor $(-1)^{(n_d+v)/2}$. The phase convention chosen here is in line with most numerical codes and corresponds to the one used in [21, 23].

Following the same procedure as used in ref [23] one obtains then for the mixing Hamiltonian the following tensorial character with respect to U(6), SU(3) and O(3):

$$\hat{H}_{mix} \;=\; (\alpha + \frac{2}{\sqrt{5}}\beta)\; T^{[2](4,0)0} \;+\; (\frac{2}{\sqrt{5}}\alpha - \beta)\; T^{[2](0,2)0} \quad . \tag{8}$$

The tensorial character of the mixing Hamiltonian inhibits the contribution of the second term to the mixing of the lowest intruder band which has the SU(3) labels $(\lambda, \mu) = (2N + 4, 0)$. Thus for this lowest band a situation similar to the one found for the U(5)-O(6) mixing arises and the mixing depends only on a particular linear combination of the parameter α and β.

Using the transformation bracket given above one can analytically study the coupling of the intruder SU(3) ground state configuration with the lowest U(5) states ($n_d = 0, L = 0$ and $n_d = 2, L = 0$), given by

$$\begin{aligned} &\langle [N] n_d = 0, 00 \mid \hat{H}_{mix} \mid [N+2](2N+4, 0)00 \rangle \\ &\quad = (\alpha + \frac{2}{\sqrt{5}}\beta) \sqrt{\frac{(N+1)(N+2)(2N+5)}{3^{N+2}}} \quad , \end{aligned} \tag{9}$$

and

$$\begin{aligned} &\langle [N] n_d = 2, 00 \mid \hat{H}_{mix} \mid [N+2](2N+4, 0)00 \rangle \\ &\quad = (\alpha + \frac{2}{\sqrt{5}}\beta) \sqrt{\frac{2(N-1)N(N+1)(N+2)(2N+5)}{5 \cdot 3^{N+2}}} \quad , \end{aligned} \tag{10}$$

respectively. Thereby we have used the matrixelements of the operators $(s^+ s^+)^{(0)}$ and $(d^+ d^+)^{(0)}$ in the U(5) basis as derived in ref. [21, 24]. In fig. 3 we show the dependence of the mixing on the boson number. The coupling with the regular ground state ($n_d = 0, L = 0$) smoothly decreases with boson number, while the coupling with the ($n_d = 2, L = 0$) two-phonon state peaks at boson number N=4.

2.3 Basic features of the U(5)-SU(3) model

Since for the other states no simple expansion can be given analytically , use was made of a numerical method to obtain the coupling matrix elements starting from the NPBOS-NPMIX codes [25, 26]. Parameters have been chosen such as to reproduce Hamiltonians that have U(5) and SU(3) symmetry respectively. The relations, connecting the more general IBM-2 NPBOS parameters to those for Hamiltonians describing an exact symmetry have been given in appendix B of part II.

In the present U(5)-SU(3) study, we have used the following Hamiltonians:

$$\hat{H}(U(5)) = \epsilon \hat{n}_d + \kappa' \hat{L} \cdot \hat{L} + a \hat{M} \quad , \tag{11}$$

$$\hat{H}(SU(3)) = \kappa \hat{Q} \cdot \hat{Q} + \kappa' \hat{L} \cdot \hat{L} + a \hat{M} \quad , \tag{12}$$

with for the U(5) limit ϵ = 0.68 MeV, κ' = -4 keV (including a small quadrupole perturbation $\Delta\kappa$ = -0.25 keV to split degeneracies in the numerical study) and for the SU(3) limit κ = -8 keV, κ' = 22 keV and $\chi = -\sqrt{7}/2$ (including similarly a small d-boson energy perturbation $\Delta\epsilon$ = 2 keV) These parameters were taken from the calculation aiming at the description of the low-lying regular and intruder excitations in the $^{192-200}$Po isotopes using this U(5)-SU(3) coupling scheme (see section 3.2). The restriction to fully symmetric F-spin configurations has been performed through an adequate choice of the Majorana strength; we considered the value a = 10 MeV. In this case we present the coupling ma-

trix elements so obtained with $\alpha = \beta = 0.15\sqrt{6/(N+1)(N+2)}$ MeV[1] with N the total boson number[2] in fig. 4 and this for N=9 and L=0,2,3,4,6 and 8 always considering the four lowest levels in both the U(5) and SU(3) dynamical symmetry. From the figure, one can see that a non-selective coupling arises, although a preferential coupling of the SU(3) ground band ($(\lambda,\mu) = (22,0)$) and the SU(3) β band ($(\lambda,\mu) = (18,2)$) to U(5) states with lower seniority, increasing with d-boson number is present. For the SU(3) γ band ($(\lambda,\mu) = (18,2)$) coupling to states with higher seniority is favoured.

In fig. 5 we then show the effect of this mixing on the regular and intruder configurations when the dynamical symmetries, as illustrated in fig. 2 have been used to obtain the unperturbed energy spectra. This mixing is of course largely determined by the energy difference of the unperturbed configurations, considering the fact that the U(5)-SU(3) mixing is not very selective, contrary to the U(5)-O(6) mixing situation. This is nicely illustrated by the relatively strong mixing of the $4_2^+, 4_4^+, 6_2^+$ and 8_2^+ states resulting from close lying unperturbed regular and intruder configurations.

We also present, albeit in a schematic way using the U(5) and SU(3) Hamiltonians as given in eqs. (11) and (12), how the U(5) and SU(3) E2 decay pattern becomes modified through the mixing. Use was made of the numerical codes NPBEM-BEMIX [25, 26]. In fig. 6a we show the unperturbed U(5) and SU(3) energy spectra but now in compressed form (left-hand side) and the energy spectrum after diagonalizing the mixing matrix of eq. (4) (right-hand side). On the left-hand side of fig. 6b we show the "unperturbed" U(5) and SU(3) B(E2) values (with arrows of which the thickness is proportional to the B(E2) value), only indicating the lower part of the SU(3) band. The mixed B(E2) decay pattern is illustrated in the middle part and on the right-hand side of fig. 6b for $\alpha = \beta$ and $\alpha = 2\beta$ respectively (with $\beta = 0.15\sqrt{6/(N+1)(N+2)}$ MeV)[3]. As stated before, most low-lying states are not much affected by the mixing and therefore the E2 decay properties are well preserved within the regular and intruder bands. Some smaller transitions occur in addition, mainly from the 4_2^+ and 4_4^+ states, where mixing does occur due to the proximity in unperturbed energy. In general one expects that the overall E2 decay properties will remain quite well intact, although accidental close-lying levels in the two subspaces can disturb the features locally. From comparison of the middle and the right part of fig. 6b, one can see clearly that the energy spectrum and E2 decay properties are not very sensitive to the relative mixing-parameter values, as was already stated earlier.

2.4 Relation to more realistic calculations

When trying to proceed from the pure U(5)-SU(3) coupling towards more realistic calculations, one should bear in mind that experimental energy spectra rarely fulfil the conditions of a dynamical symmetry. Indeed quite often the energy spectra in the separate subspaces (N, N+2) show deviations from the pure dynamical U(5) and SU(3) symmetries and one

[1] We have also performed a similar calculation with $\alpha/2 = \beta = 0.15\sqrt{6/(N+1)(N+2)}$ MeV but this doesn't affect the general conclusions of this study. Although the mixing is generally slightly enhanced, the variation of the matrix elements throughout the basis and with angular momentum is not altered qualitatively.

[2] The N-dependence of the mixing parameters results from the IBM-1 form of the mixing Hamiltonian (3), whereas in reality the mixing only involves proton excitations [2].

[3] In this schematic study, an effective charge of $e_\pi = e_\nu = 1.0$ e.b. is used for simplicity and the conclusions are therefore qualitative only.

has to go beyond this simple coupling scheme and diagonalise more realistic IBM Hamiltonians in the separate subspaces.

(i) The smaller space, characterized by N bosons, is then built by the eigenstates that are expanded using a U(5) basis. So we obtain

$$\mid J_i, N\rangle = \sum_k c^{ik}(U(5)) \mid \{U(5)\}k, N\rangle \quad . \tag{13}$$

(ii) In the second subspace containing the intruder states which are characterized by N+2 bosons, we expand the eigenstates in the SU(3) basis and obtain the states

$$\mid J_j, N+2\rangle = \sum_\ell c^{j\ell}(SU(3)) \mid \{SU(3)\}\ell, N+2\rangle \quad . \tag{14}$$

Subsequently we determine the mixing matrix elements of the Hamiltonian (3) as follows

$$\begin{aligned} &\langle J_j, N+2 \mid \hat{H}_{mix} \mid J_i, N\rangle \qquad = \\ &\textstyle\sum_{k,\ell} c^{j\ell}(SU(3))c^{ik}(U(5)) \ \langle\{SU(3)\}\ell, N+2 \mid \hat{H}_{mix} \mid \{U(5)\}k, N\rangle. \end{aligned} \tag{15}$$

The deviations of the matrices c(U(5)) and c(SU(3)) from unit matrices express the deviations from the dynamical U(5) and SU(3) symmetries, respectively. In the expression (15) the latter mixing matrix elements are the ones derived from the pure U(5)-SU(3) coupling. In matrix form the final energy matrix that needs to be diagonalised becomes

$$\left(\begin{array}{c|c} E(J_i,N) & \sum \underline{c}(U(5))\underline{c}(SU(3)) \\ & \langle\{U(5)\} \mid \hat{H}_{mix} \mid \{SU(3)\}\rangle \\ \hline \sum \underline{c}(U(5))\underline{c}(SU(3)) & \\ \langle\{U(5)\} \mid \hat{H}_{mix} \mid \{SU(3)\}\rangle & E(J_j,N+2) \end{array}\right) , \tag{16}$$

which is one step more realistic than the energy matrix of equation (4). To illustrate the effect when going away from the dynamical symmetry limit, we calculated the mixing matrix elements of the intruder states with the regular states for each lowest excitation of angular momentum L=0 to 8. Thereby the SU(3) symmetry is broken by a term $\epsilon\hat{n}_d$, with ϵ varying from 0.0 to 0.5 MeV. This is illustrated in fig. 7a. We immediately observe a very strong increase of the mixing, especially for low angular momenta. When going towards the O(6) dynamical symmetry, varying χ from $-\sqrt{7}/2$ to 0, the increase of the mixing is much smaller and is more or less independent of angular momentum. This is illustrated in fig. 7b.

Even more realistic calculations can be performed by explicitly taking into account the proton-neutron character of the various configurations within an IBM-2 configuration mixing approach [27]. Restriction to a symmetric particle-hole character is however implicitly considered in this approach. The p-h and π-ν degrees of freedom are explicitly taken into account when describing a more complete EIBM-2. Results are presented in ref. [28].

3 Application to the Po isotopes

3.1 The I=3/2 multiplet

As was discussed extensively in previous papers of this series [1]-[3], the existence of I-spin multiplets, albeit approximately, indicates that I spin is a good quantum number, i.e., I spin is a dynamical symmetry. This symmetry is related to changing a 'particle'-like boson into a 'hole'-like boson (or the other way around) in the boson wave function. From ample evidence in the Z=50 and Z=82 region, one can conclude that locally this symmetry can be broken through mixing between regular and intruder excitations.

In the case of the Po isotopes, the $[\pi(4p-2h)]$ intruder excitations should belong to the I=3/2 multiplet involving the Os $[\pi(6h)]$ regular excitations. From earlier studies [20] it became clear that the intruder band in the Po isotopes is locally affected by strong mixing with the regular excitations, especially for the lighter isotopes. Hence, in these cases I spin is no longer a good quantum number and the multiplet picture will be severely disturbed. In fig. 8 we show the comparison of the data and a two-state model calculation [20], where the unperturbed intruder energies have been reconstructed, starting from α-decay hindrance factors [19, 30] to determine the mixing of regular and intruder 0^+ configurations and using Potential Energy Surface (PES) calculations [31] as a guide to the relative position of the unperturbed 0^+ states. It is very clear that the I-spin dynamical symmetry is restored when de-mixing regular and intruder configurations. The most striking example are the 2^+ excitations in ^{196}Po, indicated by dashed lines, which energies deviate both substantially from the 2^+ energy in ^{188}Os. For ^{192}Po, where the intruder band is most probably becoming the ground band, as supported by PES calculations [31], the picture is worse. However here, no de-mixing was possible since no excited states are known experimentally. Therefore the excited band members are assumed to be pure intruder excitations. The de-mixing of the ground state as deduced from α-decay hindrance factors [19, 30] leads to a 60 keV shift of the energy, as indicated by the dashed line.

3.2 A U(5)-SU(3) coupling calculation

In the framework of the IBM-1, we have performed mixing calculations:

We describe the regular states by the $U(5)$ Hamiltonian (11) where the parameters $\epsilon = 0.68$ MeV and $\kappa' = -4$ keV have been fitted to the yrast and yrare $J^\pi = 0^+, 2^+, 4^+$ states of $^{202-208}$Po, and have been kept constant for the description of the whole series of $^{192-208}$Po isotopes. The regular yrast $6^+, 8^+$ states have a rather pure $(\pi h_{9/2})^2$ character, although, as the neutron number decreases, the 6^+ state becomes more vibrational. Thus, when restricting the calculation to the lighter $^{192-200}$Po isotopes, where the intruder excitations really start to play an important role in the low-energy spectrum, one can assume the $U(5)$ description of the regular excitations to be satisfactory up to angular momentum 6.

The intruder states are described by an $SU(3)$ Hamiltonian (12) where the parameters $\kappa = -8$ keV and $\kappa' = 22$ keV have been fitted to the ground and γ band of ^{190}Os, and kept constant throughout the whole series of $^{192-200}$Po isotopes. The parameter Δ was fitted to the excitation energy of the known intruder 0^+ levels and also kept constant for all isotopes considered, in accordance with its physical meaning. As a result, the intruder 0^+ configuration becomes the ground state in ^{192}Po as can be seen from fig. 9a.

We then introduce the mixing as described in eqs. (3) and (4), with mixing parameters $\alpha = \beta = 0.15\sqrt{6/(N+2)(N+1)}$MeV, with N the total number of bosons, which is again in line with values used earlier in this mass region [32, 33]. In the case of a pure U(5)-SU(3) dynamical symmetry coupling, the systematics and the general features of the spectra of the $^{192-200}$Po isotopes are reproduced qualitatively, but the mixing is underestimated quantitatively, especially in ^{194,196}Po. Moreover, the ground state in ^{192}Po is almost purely $\pi(4p-2h)$ in nature, in accordance with the PES predictions [31], but in disagreement with α-decay hindrance factors [19, 30] which point to mixing. It should also be noted here that these mixing calculations show that the two-state model used in [20], albeit too simple an approach, is a valid first approximation to disentangle regular and intruder components since the lowest-lying unperturbed states are indeed the dominant components for the experimentally known levels. This can be clearly seen from figs. 11-15.

3.3 A more realistic IBM-1 mixing calculation

In this calculation we start from the I-spin concept and adapt for the description of the intruder states in the Po isotopes a more general Hamiltonian, suitable for the description of the ground and γ bands in the corresponding Os isotopes,

$$\hat{H} \;=\; \epsilon\hat{n}_d + \kappa\hat{Q}\cdot\hat{Q} + \kappa'\hat{L}\cdot\hat{L} + \Delta \quad , \tag{17}$$

and which is similar to the one used for an earlier calculation of $^{174-180}$Os [34]. The parameters $\epsilon = 0.22$ MeV and $\chi = -0.8$ are kept constant for all isotopes, while κ, κ' are smoothly varying for $^{184-192}$Os ($^{192-200}$Po). Their values are in line with those used in [34] as is illustrated in fig. 10. The parameter Δ was again fitted to the excitation energy of the known intruder 0^+ levels and also kept constant for all isotopes considered. As a result the intruder 0^+ configuration becomes nearly degenerate with the regular ground state in ^{192}Po, as indicated in fig. 9b. For the more general Hamiltonian of eq. (17), the mixing results are in fair overall agreement with experimental data, as can be seen from figs. 11-15. The ground state in ^{192}Po is now mixed, but with the regular configuration as the dominant one. For both calculations, one observes disagreement between the experimental and calculated yrast 8^+ level, as neutron number increases. This is linked with the dominant regular nature of this state, which, as a $(\pi h_{9/2})^2$ configuration [11, 12, 20], is outside the IBM model space.

As an example, we have calculated the electric quadrupole transition probabilities for the low-lying excitations in ^{194}Po, where mixing is rather important[4]. Results are shown in fig. 16. By comparing the unperturbed and mixed B(E2) transition probabilities, one observes that the pattern of existing transitions remains at least qualitatively, with some additional non-negligible transitions between (dominantly) intruder and (dominantly) regular states. This is even more clear when looking at the intruder and regular components of the mixed states, as shown in fig. 12.

[4]The ratio of effective charges for the N+2 boson space versus the N boson space is 0.8, in accordance with the value used for ^{190}Hg [32]. Furthermore, we have taken $e_\pi = e_\nu = e$ to be equal to 1. The relative strength of the transitions will not be altered by introducing an effective charge $e = 0.13$ or 0.17 e.b. already used in this mass region [32, 34, 35].

4 Conclusions

In the present paper we have discussed the U(5)-SU(3) coupling scheme, which has been studied both analytically and numerically. One finds a non-selective and rather small coupling, resulting in only minor changes in the energy spectrum and electric quadrupole transition probabilities, mainly induced accidentally due to small energy spacings between unperturbed levels. We have shown that this scheme is applicable to the Po isotopes, albeit approximately, and have compared the results so obtained with a more realistic IBM-1 calculation. In this way one obtains a consistent description of the low-energy spectrum of $^{192-200}$Po, with an interpretation in terms of mixed regular and intruder $\pi(4p-2h)$ excitations, in line with an independent study performed in ref. [20]. The Po isotopes moreover constitute themselves a nice illustration of the I-spin concept. Once the local mixing of intruder and regular states is excluded from the picture, one recovers the I=3/2 multiplet approximately. Hence one can conclude that globally the particle-hole boson symmetry, with corresponding quantum label I spin, holds at least approximately. In an algebraic language, within the particle and hole boson space, U(12) is a dynamical symmetry algebra, although locally this symmetry can be broken through mixing of regular and intruder states, which are characterized by different I-spin quantum labels. The resulting states do not have good I-spin anymore, even though for weak mixing, the I-spin classification scheme is still approximately valid.

With the present paper we have finished the detailed (analytical and numerical) study of how the appearance of two different dynamical symmetries in a single nucleus can be described (U(5)-O(6) (II), O(6)-SU(3) (III) and U(5)-SU(3) (IV)). We have discussed the idea of intruder spin (related to changing particle-like into hole-like bosons and vice versa) which has been introduced in [36] and was studied in depth in (I) in both the Z=50 and Z=82 region as a rather valuable guidance principle for studying systematics of low-lying nuclear excitations.

From the vertical classification scheme and the K-spin concept, we have learned that the IBM mixing calculations - as introduced already earlier [27] and used subsequently in several studies of shape coexistence - can be viewed as limiting cases of the general algebraic structure. Thereby, the description of regular and intruder states by different Hamiltonians points to K-symmetry breaking.

These findings are a good starting point for further studies in which particle-hole and proton-neutron degrees of freedom are treated on equal footing in an EIBM-2 model (or EIBM-3 for light nuclei). This again leads to new possible symmetries and additional classes of states [28, 37, 38].

It would be interesting to implement these results in an Extended-IBM code which then allows for further numerical studies of shape coexistence in different mass regions.

It is furthermore possible to combine the horizontal I-spin classification with the vertical K-spin classification of multi-particle-multi-hole excitations, allowing for the description of such states and the systematics of their properties in neighbouring nuclei. This also opens perspectives for the description of high-spin states and superdeformation in nuclei.

Acknowledgements

The authors are most grateful to P. Van Isacker for many discussions on the group theoretical aspects of this work. They also thank B.R. Barrett, N. Bijnens, J. Cizewski, M. Huyse, A.M. Oros. P. Van Duppen and R. Wyss for useful discussions concerning the Po isotopes. In particular the complementary studies of the Po isotopes by A.M. Oros were extremely useful to them. This work was supported by the Swiss National Science Foundation (JJ). Three of the authors (CDC, BD and KH) thank the F.W.O., I.I.K.W. and I.W.T. for financial support. Part of this work has also been supported by DOE grant DE-FG02-96ER 40958 at Georgia Tech (JLW), AC05-76OR 00033 at UNISOR and a NATO Research Grant CRG 96-0981. One of the authors (KH) is grateful to CERN for financial support in the final stage of this work.

References

[1] C. De Coster, K. Heyde, B. Decroix, P. Van Isacker, J. Jolie, H. Lehmann, and J.L. Wood, Nucl. Phys. A **600** (1996) 251.

[2] H. Lehmann, J. Jolie, C. De Coster, B. Decroix, K. Heyde, J.L. Wood, Nucl. Phys. A **621** (1997) 767

[3] C. De Coster, B. Decroix, K. Heyde, J.L. Wood, J. Jolie, H. Lehmann, Nucl. Phys. A **621** (1997) 802

[4] C. De Coster, B. Decroix, K. Heyde, Phys. Lett. B **379** (1996) 20

[5] K. Kitao, Nuclear Data Sheets **75** (1995) 99

[6] J. Rikovska, N.J. Stone, P.M. Walker and W.B. Walters, Nucl. Phys. A **505** (1989) 145 and refs. therein

[7] L.J. Jardine, S.G. Prussin, J.M. Hollander, Nucl. Phys. A **190** (1972) 261

[8] H. Beuscher, D.R. Zolnowski, D.R. Haeni, T.T. Sugihara, Phys. Rev. Lett. **36** (1976) 1128

[9] R.G. Helmer, C.W. Reich, Phys. Rev. C **27** (1983) 2248

[10] L.A. Bernstein et al., Phys. Rev. C **52** (1995) 621

[11] W. Younes et al., Phys. Rev. C **52** (1995) R1723

[12] W. Younes and J.A. Cizewski, Phys. Rev. C **55** (1997) 1218

[13] N. Fotiades et al., Phys. Rev. C **55** (1997) 1724

[14] A. Maj, H. Grawe. H. Kluge, A. Kuhnert, K.H. Maier, J. Recht, N. Roy, H. Hübel, M. Guttormsen, Nucl. Phys. A **509** (1990) 413

[15] D. Alber et al., Z. Phys. A - Hadr. and Nucl. **339** (1991) 225

[16] N. Bijnens et al., Phys. Rev. Lett. **75** (1995) 4571

[17] K. Helariutta et al., Phys. Rev. C **54** (1996) R2799

[18] N. Bijnens et al., Phys. Rev. C **58** (1998) 754

[19] N. Bijnens, PhD thesis, Leuven (1998) unpublished and refs. therein

[20] A. Oros, K. Heyde, C. De Coster, B. Decroix, R. Wyss, B.R. Barrett, P. Navratil, Nucl. Phys. A **645** (1999) 107

[21] H. Lehmann and J. Jolie, Nucl. Phys. A **588** (1995) 623.

[22] Iachello, F., and Arima, A., *The Interacting Boson Model*, Cambridge University Press, 1987.

[23] J. Jolie and H. Lehmann, Phys. Lett. B **342** (1995) 1.

[24] A. Frank and P. Van Isacker *Algebraic Methods in Molecular & Nuclear Structure Physics* ed. Wiley & Sons (1994) p.378.

[25] T. Otsuka, O. Scholten, NPBOS-NPBEM, version July 1979, manual KVI-253

[26] P.D. Duval, NPMIX-BEMIX, version 1982, private communication

[27] P.D. Duval and B.R. Barrett, Nucl. Phys. A **376** (1982) 213.

[28] B. Decroix, J. De Beule, C. De Coster, K. Heyde, A. Oros and P. van Isacker, Phys. Rev. C **57** (1998) 2329

[29] *Nuclear Data Sheets* **58**, 243 (1989), **82**, 1 (1997), **59**, 133 (1990), **61**, 243 (1990), **64**, 205 (1991)

[30] R.G. Allatt et al., Phys. Lett. B **437** (1998) 29

[31] R. Wyss, private communication (1998)

[32] A.F. Barfield, B.R. Barrett, K.A. Sage and P.D. Duval, Z. Phys. A **311** (1983) 205

[33] Harder, M., Tang, K. and Van Isacker, P., *Phys. Lett.* B **405**, 25 (1997).

[34] T. Kibédi, G.D. Dracoulis, A.P. Byrne, P.M. Davidson and S. Kuyucak, *Nucl. Phys.* A **567**, 183 (1994)

[35] R. Bijker, A.E.L. Dieperink, O. Scholten, Nucl. Phys. A **344** (1980) 207

[36] K. Heyde, C. De Coster, J. Jolie and J.L. Wood, Phys. Rev. C **46** (1992) 541

[37] B. Decroix, C. De Coster, K. Heyde, A.M. Oros, J. De Beule, Phys. Rev. C **58** (1998) 232

[38] B. Decroix, J. De Beule, C. De Coster, K. Heyde, Phys. Lett. B **439** (1998) 237

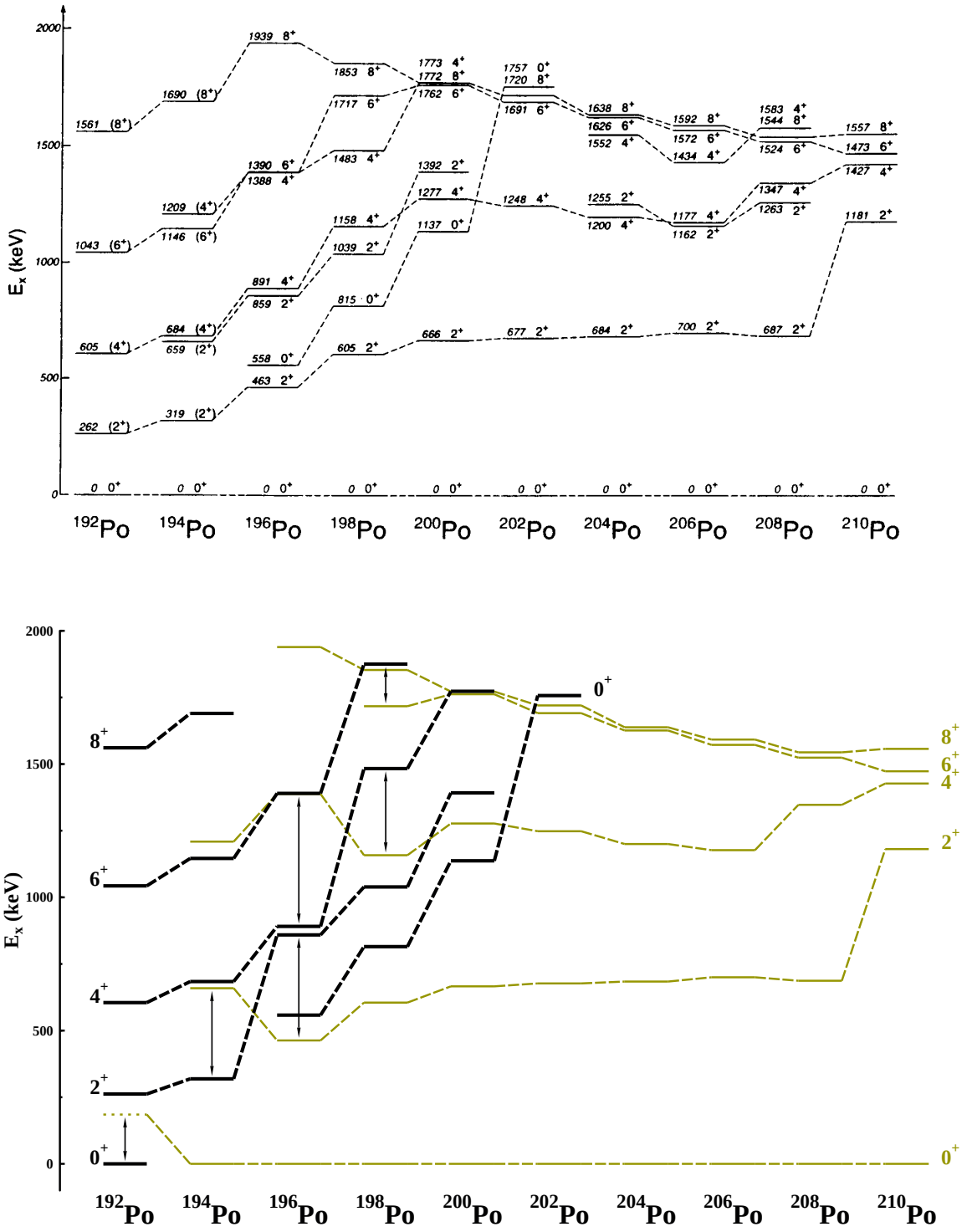

Figure 1: (a) Systematics of the light Po isotopes. Below the shell closure at N=126 with the "two-proton" nucleus ^{210}Po a "regular regime" with smooth variation of the yrast levels is observed down to ^{200}Po. The strong downsloping of the yrast levels in the isotopes below ^{200}Po can be optically associated with the strong lowering in the energy of the first excited 0^+ state. Figure taken from [12]. (b) Interpretation of the data in terms of a regular (grey) and an intruder $\pi(4p-2h)$ (black) band where mixing occurs, as indicated by the arrows. The dotted 0^+ level in ^{192}Po is an estimate of the energy based on PES calculations and α decay hindrance factors [20].

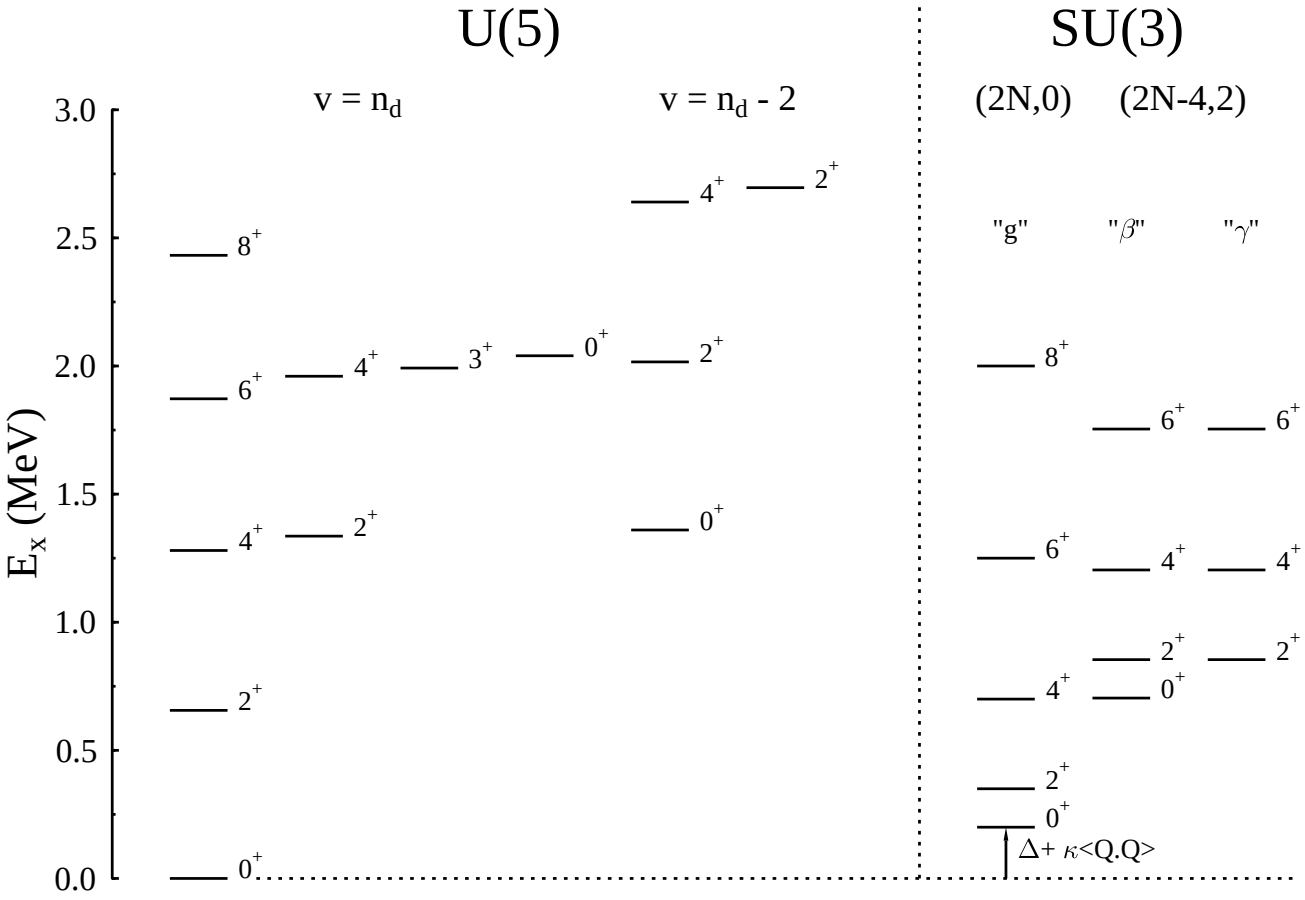

Figure 2: The unperturbed U(5) and SU(3) limit shown next to each other. The SU(3) configuration is shifted by Δ (= 2.4 MeV) and subsequently lowered by the quadrupole interaction. For the calculation the Hamiltonians (11) and (12) are used. Parameters are listed in the text.

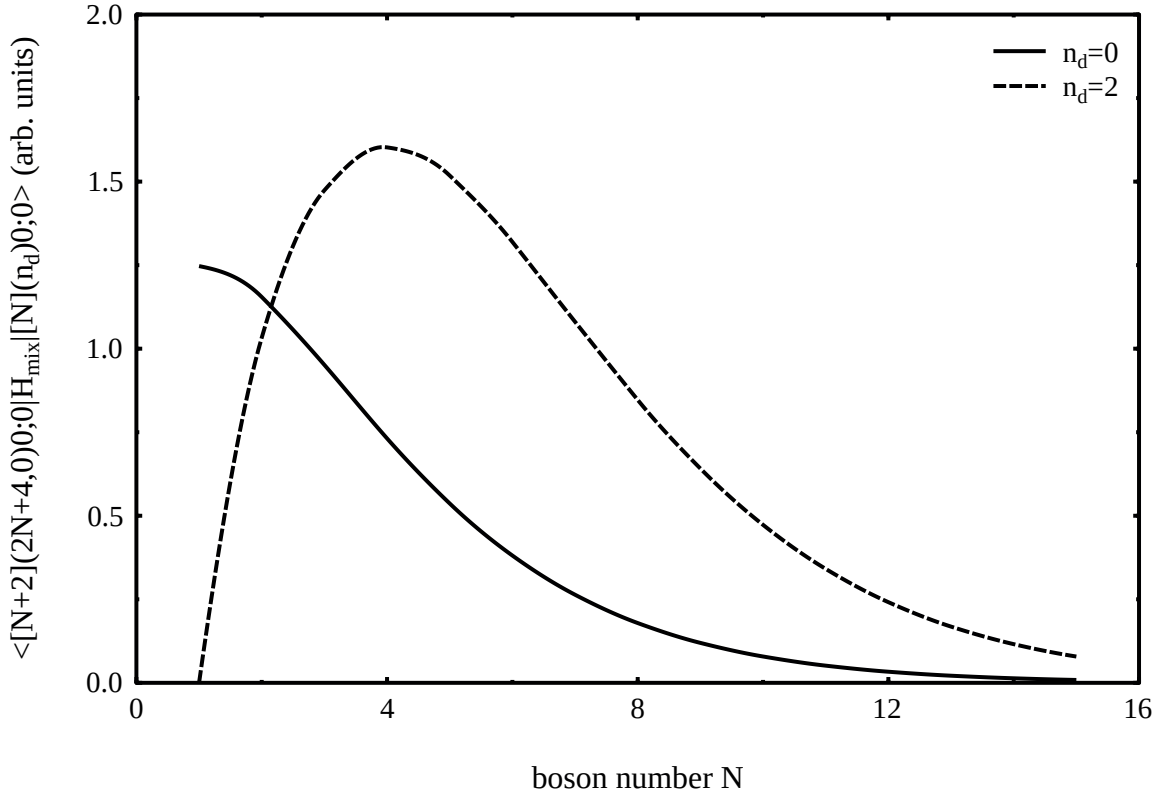

Figure 3: Absolute value of the mixing matrix elements for the SU(3) ground state and the two lowest 0^+ U(5) eigenstates, as calculated analytically. The parameter dependent factor $(\alpha + 2/\sqrt{5}\beta)$ is divided out.

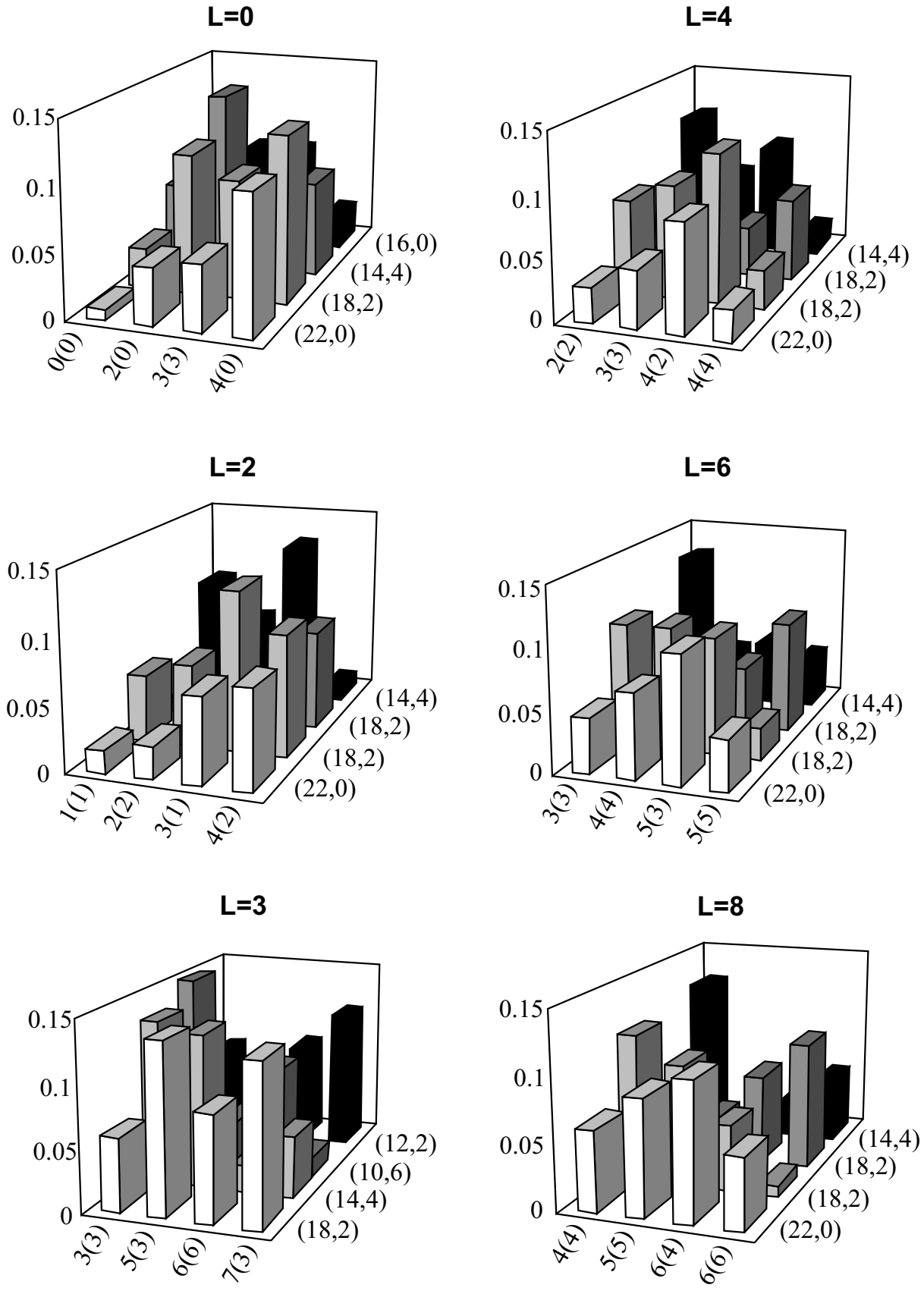

Figure 4: Absolute value of the mixing matrix elements for states of different angular momentum L, between regular U(5) configurations, indicated by their quantum numbers $n_d(v)$ and intruder SU(3) configurations, labeled by the quantum numbers (λ, μ). The parameters for the calculation are listed in the text. The mixing parameters have been chosen $\alpha = \beta = 0.15\sqrt{6/(N+1)(N+2)}$ MeV.

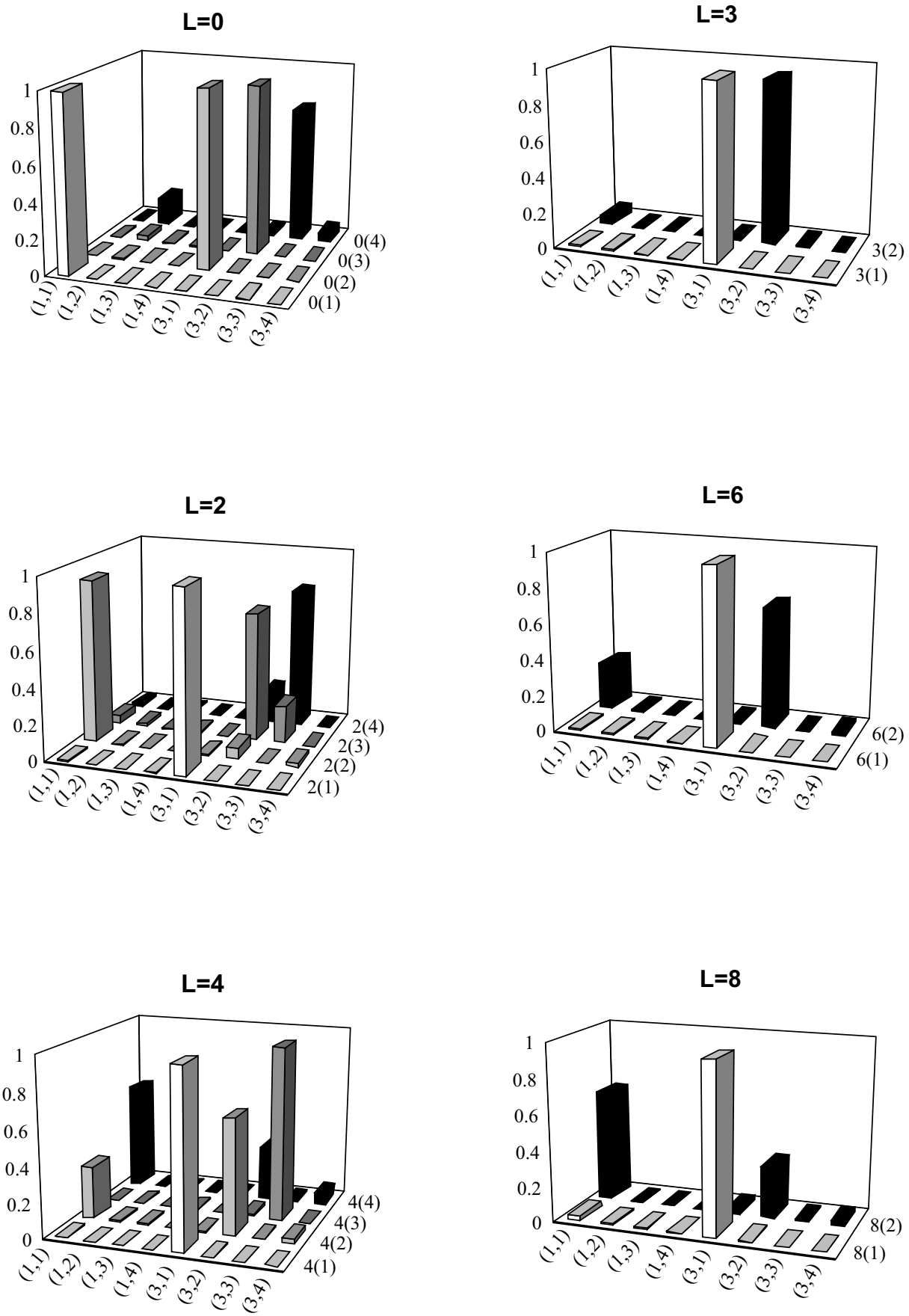

Figure 5: Square of the amplitudes of the lowest excitations with angular momentum L, indicated by the labels $L(i), i = 1, \ldots 4$ in a basis spanned by the four lowest (unmixed) regular U(5) states and intruder SU(3) states, indicated by the labels $(N_\pi, k), k = 1, \ldots 4$, where we put N_π equal to 1 resp. 3, the correct number of proton bosons when calculating

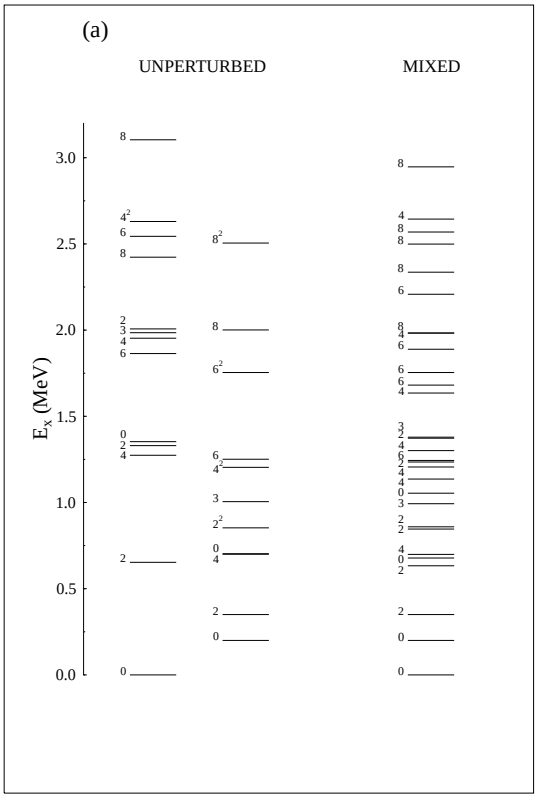

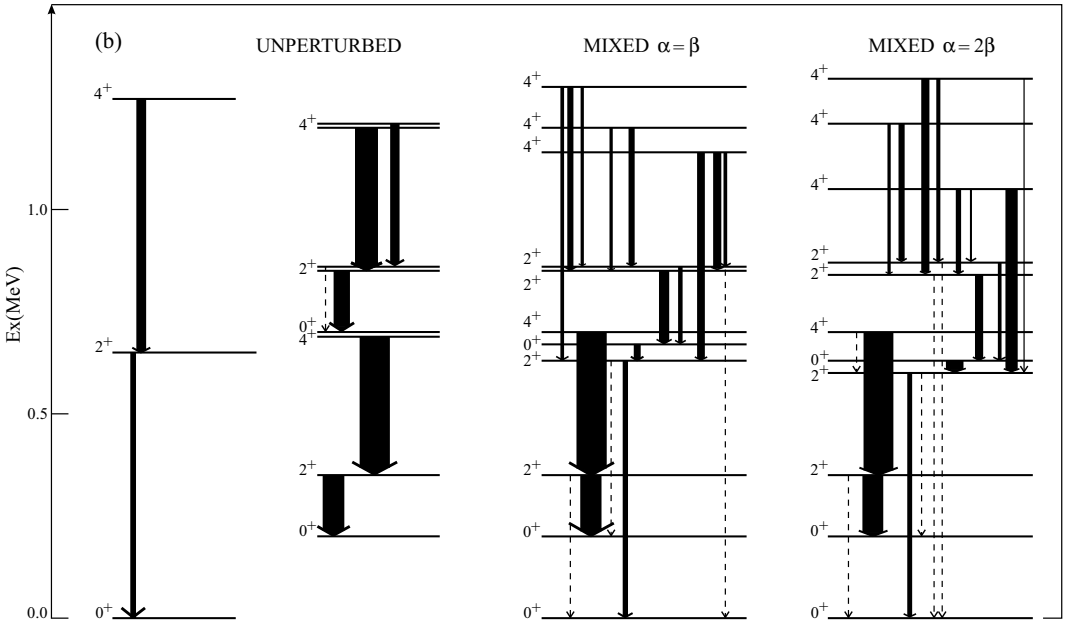

Figure 6: (a) The unperturbed U(5) and SU(3) energy spectra, now shown in compressed form (equal to fig. 2) and the energy spectrum after diagonalizing the mixing matrix of eq. (4). (b) The B(E2) reduced transition probabilities as determined in both the pure (left-hand side) U(5) and SU(3) limit, and after taking the mixing Hamiltonian into account with $\alpha = \beta = 0.15\sqrt{6/(N+1)(N+2)}$ MeV (middle part) and $\alpha = 2\beta = 0.3\sqrt{6/(N+1)(N+2)}$ MeV (right-hand side) respectively.

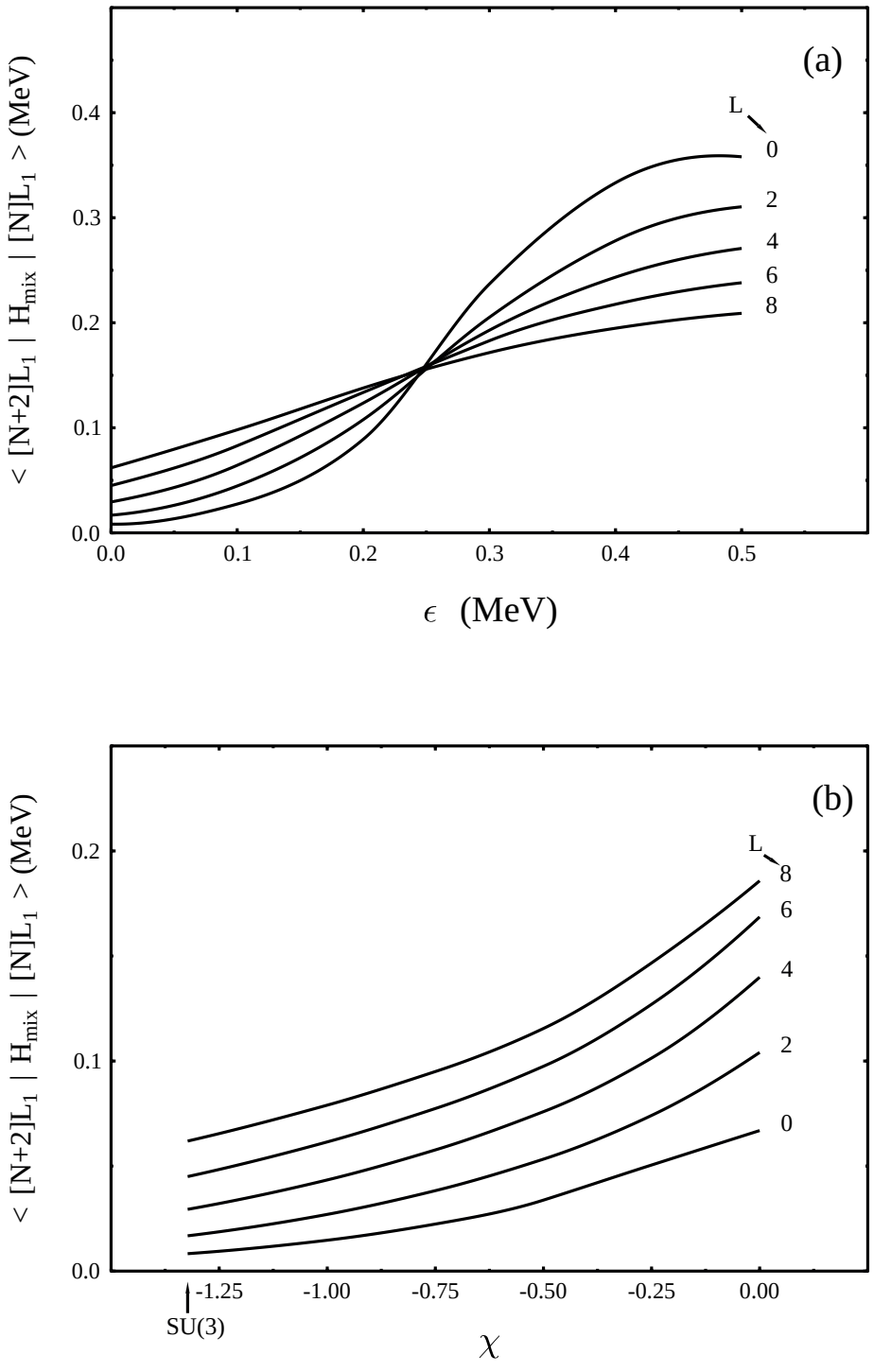

Figure 7: Mixing matrix elements between the lowest intruder and lowest regular state for angular momenta L=0,2,4,6,8, when breaking the SU(3) dynamical symmetry (a) by a term $\epsilon\hat{n}_d$ and (b) going towards the O(6) dynamical symmetry changing χ from $-\sqrt{7}/2$ to 0.

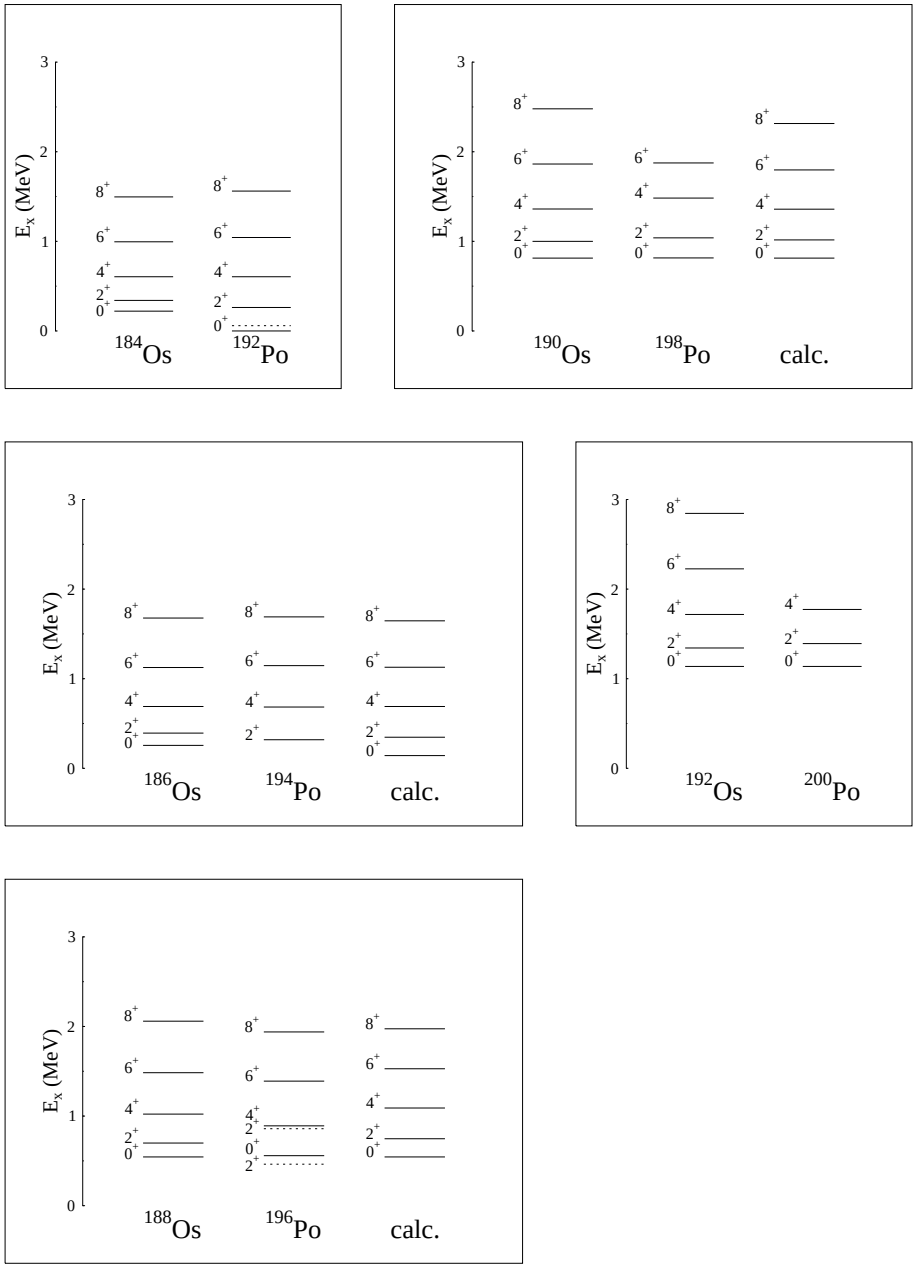

Figure 8: I=3/2 multiplet involving $[\pi(6h)]$ excitations in $^{184-192}$Os and $[\pi(4p-2h)]$ excitations in $^{192-200}$Po. Details are explained in the text. Data are taken from refs. [13, 20] for Po and ref. [29] for Os. The Os band has been normalized to the unperturbed 0^+ energy, which is very little affected by mixing, as is clear from the comparison with the Po data, except for ^{192}Po, where from α-decay the 0^+ is known to be mixed, and ^{194}Po, where the experimental 0^+ energy is unknown, and the 4^+ energy is nearly unaffected by mixing and hence used for normalization of the Os band.

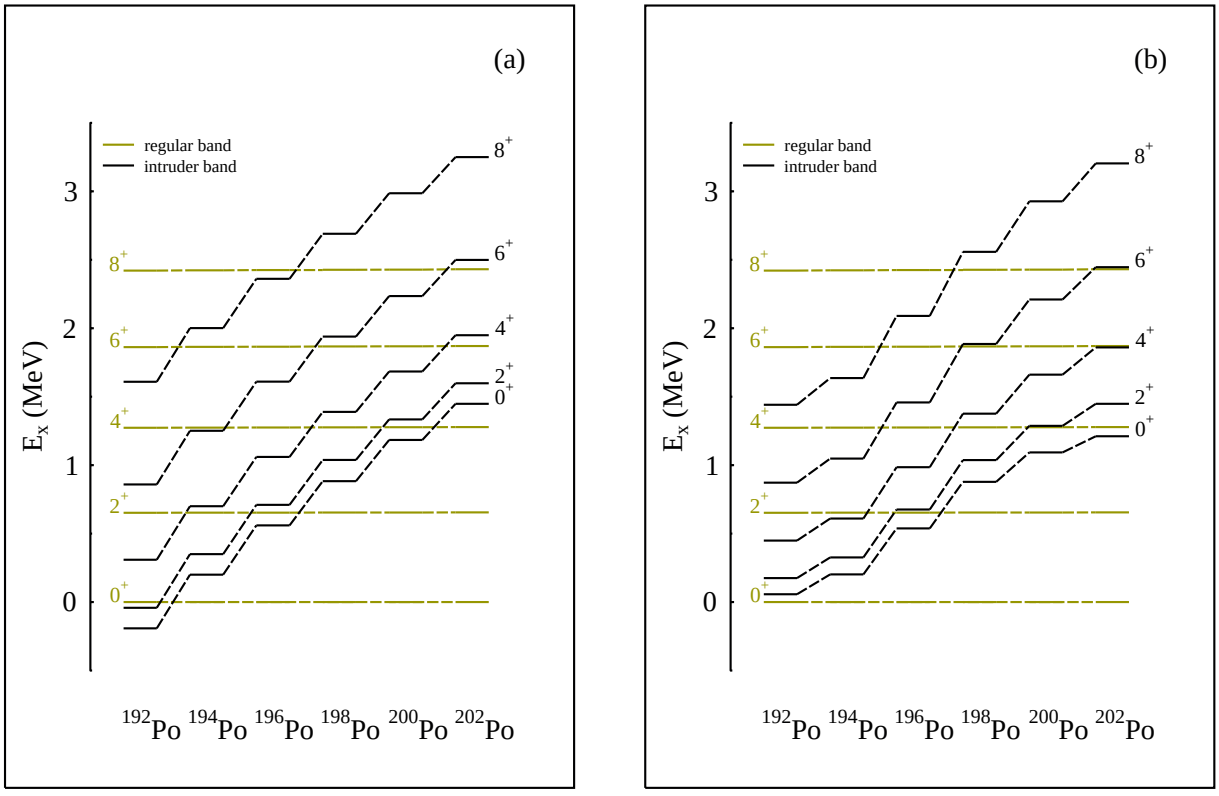

Figure 9: Unperturbed regular (grey) and intruder (black) excitations for the $^{192-200}$Po isotopes (a) for a U(5)-SU(3) mixing calculation and (b) for a more general IBM-1 mixing calculation. Details of both calculations can be found in the text.

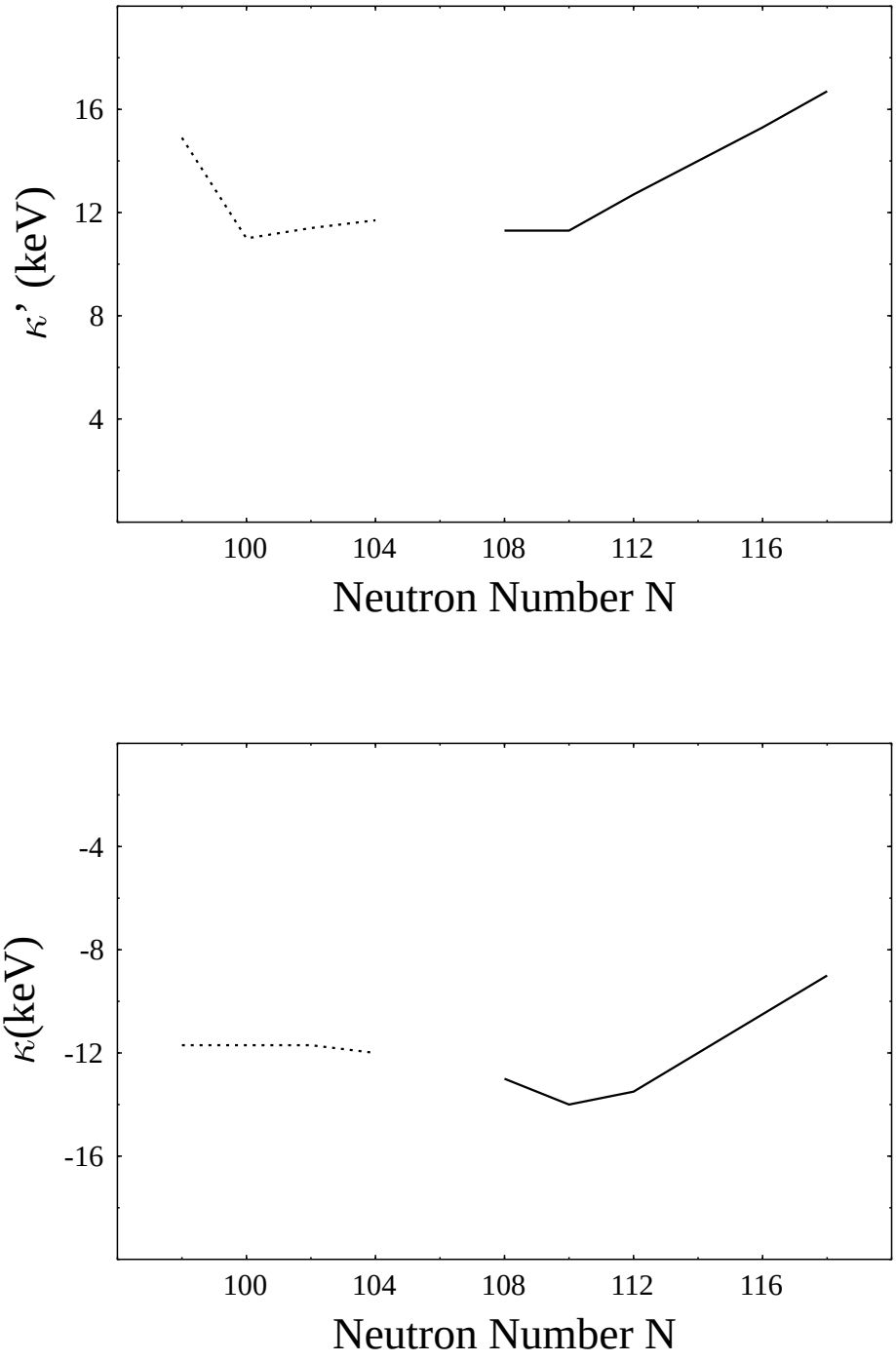

Figure 10: Value of the parameters κ and κ' as a function of neutron number. The dotted line indicates the parameterization for the lighter Os isotopes as used in [34].

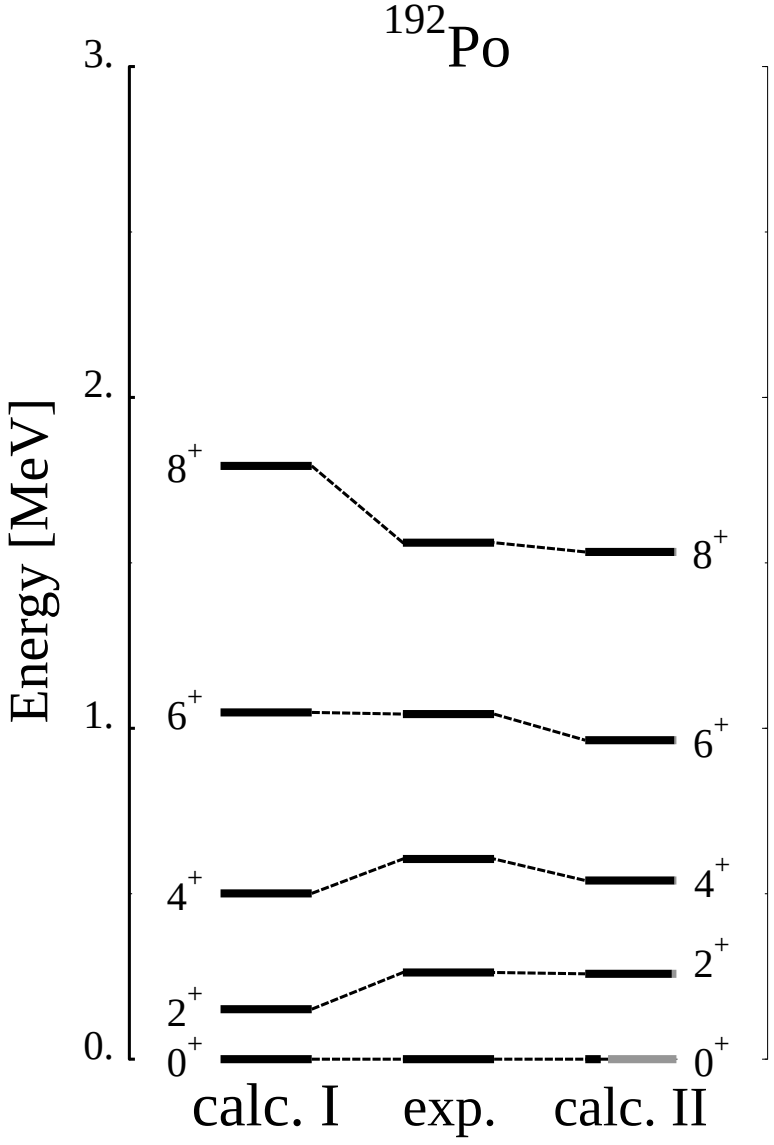

Figure 11: Results of both mixing calculations for ^{192}Po, as described in the text : the U(5)-SU(3) coupling calculation (calc. I) and the more realistic IBM-1 mixing calculation (calc. II). The relative summed contribution of regular (intruder) components to the wave functions is indicated by the grey (black) parts of the respective levels. Thereby the contribution of the lowest unperturbed level is given by a thick line. The comparison with experimental data is given in the middle column (exp.).

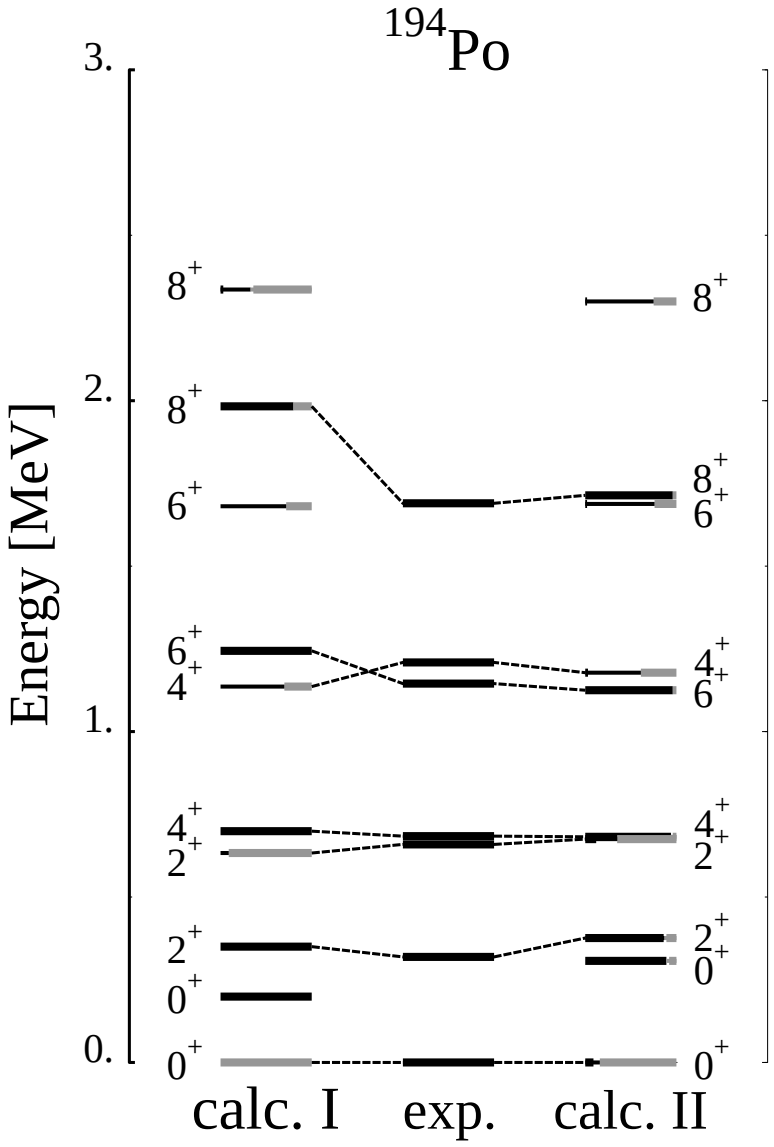

Figure 12: Similar to fig. 11, but now for ^{194}Po.

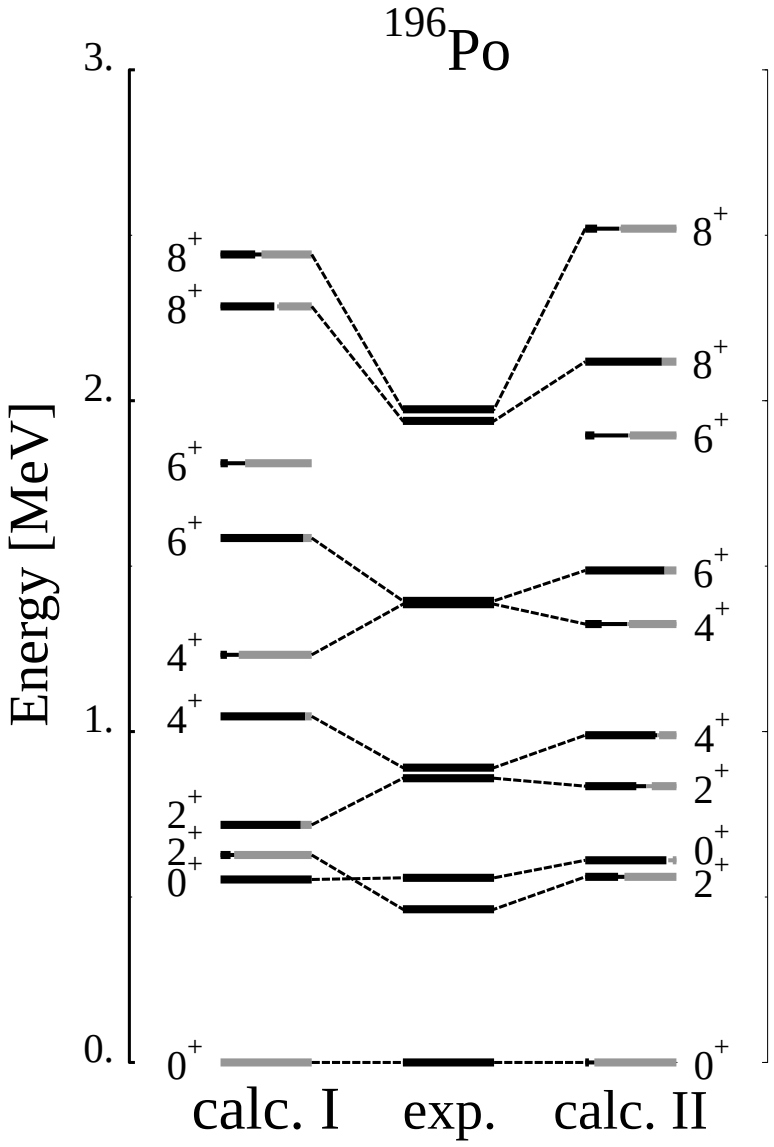

Figure 13: Similar to fig. 11, but now for ^{196}Po.

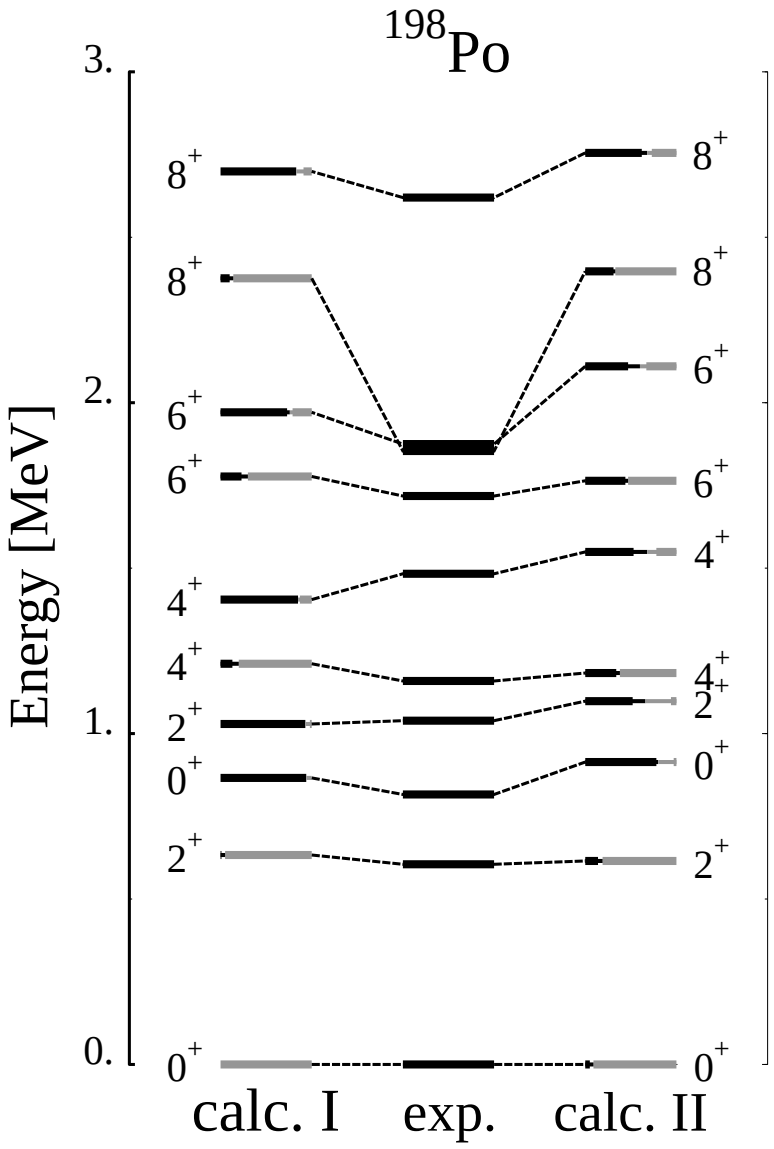

Figure 14: Similar to fig. 11, but now for ^{198}Po.

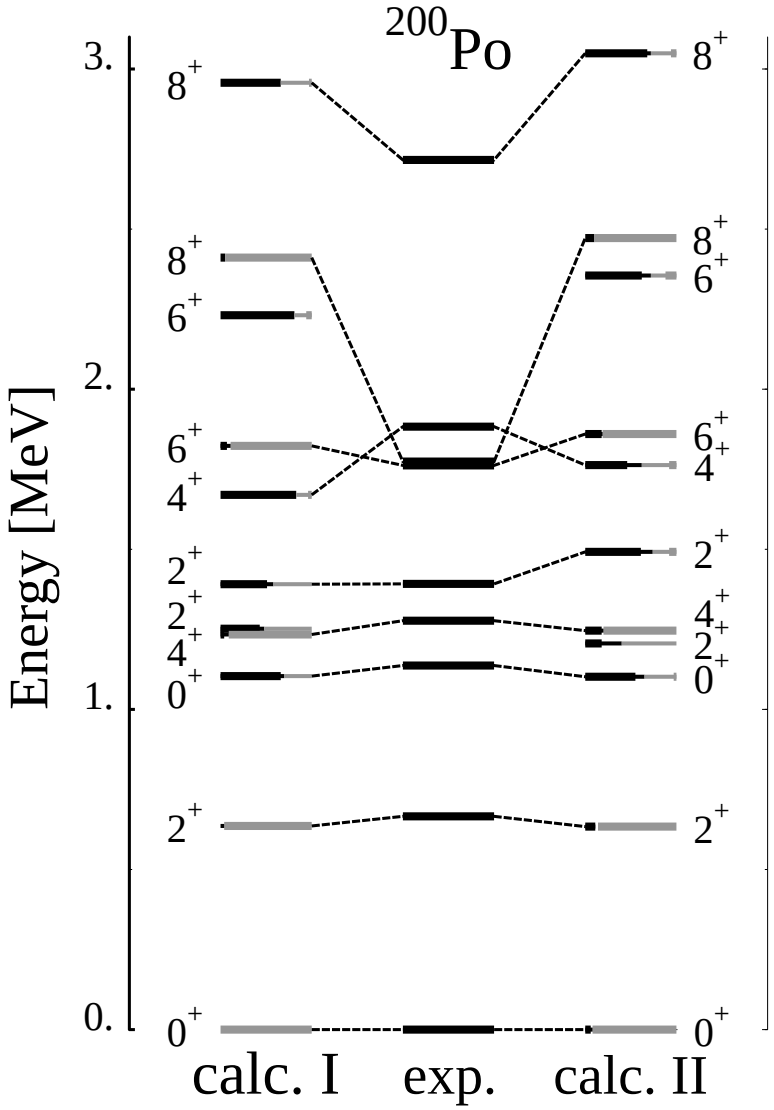

Figure 15: Similar to fig. 11, but now for ^{200}Po.

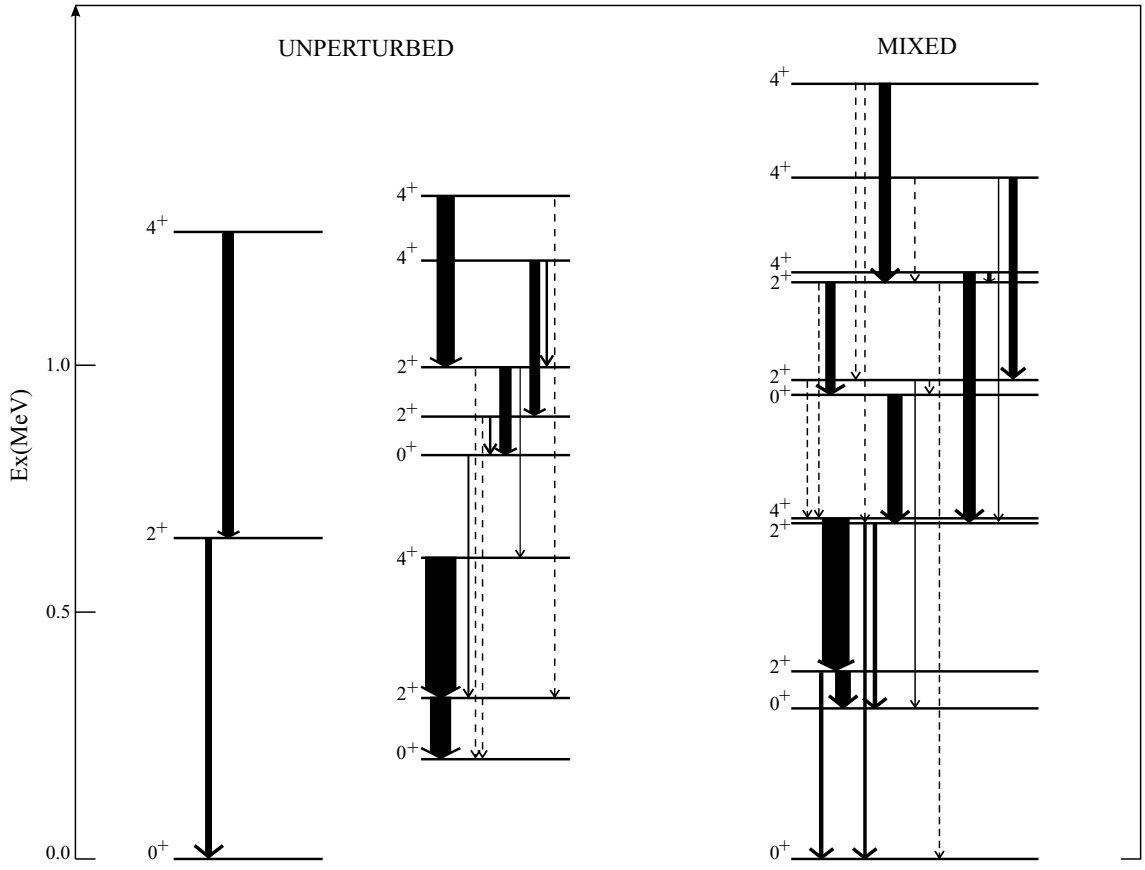

Figure 16: The B(E2) reduced transition probabilities as obtained from the more general IBM-1 mixing calculation for ^{194}Po. Both the unperturbed values and the results after mixing are shown.